Aus dem Institut für medizinische Immunologie
der Medizinischen Fakultät Charité – Universitätsmedizin Berlin

DISSERTATION

Mitochondrial damage and axon degeneration in chronic neuroinflammation

zur Erlangung des akademischen Grades
Medical Doctor - Doctor of Philosophy (MD/PhD)

vorgelegt der Medizinischen Fakultät
Charité – Universitätsmedizin Berlin

von

Maria Elena Bros Esqueu
aus Barcelona

Datum der Promotion: 05.06.2016

CONTENTS

SUMMARY

Abstract

Mitochondrial damage contributes to clinical deficit in a number of neuroinflammatory and neurodegenerative disorders. Mitochondria are crucial for neuronal function, as they produce most of the cellular energy. Within axons, they are transported to those areas with higher energetic demands. Increased production of reactive oxygen species during neuroinflammation can interfere with mitochondrial trafficking and function and promote axonal and neuronal pathology. However, how mitochondrial damage is initiated, and how this contributes to axonal damage and disease progression remains unknown. The primary aim of this work was to establish novel tools for monitoring and quantifying mitochondrial transport within axons. For this purpose, I established a model system for visualizing mitochondrial trafficking in myelinated axons, and determined what strategies are most adequate to quantify mitochondrial movements. By using these tools, it could then be demonstrated that oxidative stress altered both transport and function of mitochondria, and that these alterations initiated at the nodes of Ranvier. From there, mitochondrial damage progressed bidirectionally until the entire mitochondrial population was affected, which led to degeneration of axons. Oxidative damage to both mitochondria and axons could be prevented by increasing mitochondrial energetic supply. However, the antioxidant idebenone did not reduce axonal damage and disease severity in a model of chronic neuroinflammation. In conclusion, this work provides methodological advance for examining mitochondrial transport in axons, and demonstrates that the nodes of Ranvier are a key axonal structure for mitochondrial damage that should be considered to establish new neuroprotective therapies for neuroinflammatory disorders.

Zusammenfassung

Mitochondriale Schäden spielen bei verschiedenen neuroinflammatorischen und neurodegenerativen Erkrankungen eine Rolle, indem sie zu klinischen Defiziten beitragen. Mitochondrien sind wesentlich an neuronalen Funktionen beteiligt, da sie den Großteil der Energie für die Zellen produzieren, und werden innerhalb des Axons zu den Bereichen transportiert, die am meisten Energie benötigen. Doch bei Neuroinflammation und der daraus resultierenden Überproduktion von reaktiven Sauerstoffspezies kann diese Funktion und Migration der Mitochondrien beeinflusst werden, wodurch axonale und neuronale Pathologien begünstigt werden. Im Moment ist noch immer unbekannt, wie die Schäden der Mitochondrien ausgelöst werden und wie diese axonalen Schäden entstehen und zum Krankheitsprogress beitragen. Das primäre Ziel dieser Dissertation war es, neue Methoden zur Überwachung und Quantifizierung des mitochondrialen Transports innerhalb der Axone zu etablieren. Es wurde deshalb ein Modell etabliert, das die Visualisierung mitochondrialer Bewegungen in myelinierten Axonen ermöglicht. Außerdem wurden die besten Strategien zur Quantifizierung mitochondrialer Migration bestimmt. Unter Verwendung dieser Methoden konnte demonstriert werden, dass oxidativer Stress sowohl Transport als auch Funktion der Mitochondrien beeinflusst, und dass diese Veränderungen an den Ranvier-Schnürringen beginnen. Von dort breiten sich die mitochondrialen Schäden bidirektional aus, sodass am Ende die gesamte Population betroffen ist, was letztendlich zu einer axonalen Degeneration führt. Durch eine erhöhte mitochondriale Energiezufuhr konnten die oxidativen Schäden an Axonen und Mitochondrien verhindert werden. Dennoch konnte das Antioxidans Idebenone axonale Schäden und das Krankheitsausmass an einem Modell chronischer Neuroinflammation nicht reduzieren. Zusammenfassend kann gesagt werden, dass diese Arbeit ein methodischer Fortschritt ist, der zum Verständnis des mitochondrialen Transports in Axonen beiträgt und demonstriert, dass Ranvier-Schnürringe die hauptverantwortliche Struktur für mitochondriale Schäden darstellen. Sie sollten deshalb für neue neuroprotektive Therapien gegen neuroinflammatorische Erkrankungen in Erwägung gezogen werden.

Introduction

In multiple sclerosis (MS), a chronic inflammatory disease of the central nervous system (CNS), T cells directed against components of the myelin initiate an autoimmune reaction that leads to demyelination and axonal damage (Lucchinetti et al., 2000; Sawcer et al., 2011). During the first few years of disease, most patients present with periods of neurological disability followed by periods of recovery (relapsing–remitting MS, RRMS). As the disease progresses, the clinical recovery between episodes becomes incomplete, leading to a gradual neurological deterioration (secondary progressive MS, SPMS) (Lublin and Reingold, 1996; Scalfari et al., 2010). Most current therapies for MS target exclusively the immune aspects of the disease and are effective in reducing the number and the frequency of clinical relapses, but do not influence disease progression (Wingerchuk and Carter, 2014).

The worsening of neurological function in MS correlates with damage to the axons (Trapp et al., 1998). Although the cause of axonal damage is not known, the finding that some patients with mitochondrial DNA mutations developed an MS-like disease suggested that mitochondrial damage was involved in MS pathogenesis (Harding et al., 1992; Jansen et al., 1996; Horvath et al., 2000). More recent investigations demonstrated that mitochondrial alterations are present in early stages of MS (Mahad et al., 2008; Mahad et al., 2009; Witte et al., 2009), and even precede axonal degeneration in experimental MS models (Qi et al., 2006; Nikic et al., 2011). Thus, mitochondrial damage has been increasingly considered a major determinant of axonal degeneration in MS (Lassmann et al., 2012; Campbell et al., 2014; Friese et al., 2014).

Mitochondria have crucial functions for the cells: they produce energy, regulate calcium homeostasis and signal apoptosis. Within axons, mitochondria are transported from the cell body— where they are presumably synthesized—along microtubules and actin filaments to distal areas (Saxton and Hollenbeck, 2012). Both mitochondrial transport and function are essential for axonal viability (Chang and Reynolds, 2006; Schon and Przedborski, 2011; Sheng and Cai, 2012), and their disruption leads to energetic failure and neurodegeneration (Trushina et al., 2004; Stokin et al., 2005; Chang et al., 2006; De Vos et al., 2007).

In chronic CNS inflammation, activated immune cells persistently release reactive oxygen species (ROS) into the infiltrated brain and spinal cord (Glass et al., 2010; Nikic et al., 2011). While small amounts of ROS are necessary for a number of physiological processes, excessive oxygen radicals become toxic to organelles (Lin and Beal, 2006). Increased levels of oxidative stress might therefore contribute to mitochondrial damage and subsequent degeneration of axons (Fang et al., 2012). Thus, understanding mitochondrial function and dynamics in health and pathology might provide key insights into the pathogenesis of neuroinflammatory disorders. However, how oxidative stress damages mitochondria, and how this contributes to axonal damage and disease progression remains unknown. Moreover, mitochondrial movements are complex, which makes both monitoring and quantifying mitochondrial transport technically challenging. Simplified yet reliable tools for tracking mitochondria within axons need to be established.

Objectives

The overall goal of this thesis was to elucidate the contribution of oxidative stress and mitochondrial dysfunction in axonal damage in experimental setups, with the ultimate aim of finding effective neuroprotective therapies for progressive MS.

The specific objectives were the following:

1. To establish novel tools for monitoring and quantifying mitochondrial dynamics in neurons

    1.1 To establish a simplified yet reliable model system to image mitochondrial transport within myelinated axons

    1.2 To determine the suitability of manual and automated methods for tracking mitochondria within axons

2. To investigate how oxidative stress damages mitochondria in axons and contributes to axon degeneration

3. To examine the efficacy of the antioxidant idebenone as a neuroprotective strategy *in vivo* in an experimental model of chronic neuroinflammation

Methods

All experimental procedures involving mice were approved by the regional animal study committee of Berlin (*Landesamt für Gesundheit und Soziales* Berlin). Animal work was conducted in accordance with the European Communities Council Directive of 24 November 1986 (86/609/EEC).

All methods are described in detail in Fiebiger et al., 2013; Bros et al., 2014; Bros et al., 2015a and Bros et al., 2015b.

Preparation of explanted roots and primary cortical neurons

Ventral roots were explanted from adult C57BL/6 and B6.Cg-Tg(Thy1-CFP/COX8A)S2Lich/J mice. The dorsal spinal column was exposed and the vertebrae were cut laterally from rostral to caudal. The spinal cord was then sectioned at the thoracic level, and gently lifted up to expose the roots. The roots were cut distal to the spinal cord, before forming the peripheral nerves, and placed in cold artificial cerebrospinal fluid (aCSF; in mM: 124 NaCl, 1.25 NaH_2PO_4 x H_2O, 10 Glucose x H_2O, 1.8 $MgSO_4$, 1.6 $CaCl_2$ x $2H_2O$, 3 KCl and 26 $NaHCO_3$). aCSF was continuously oxygenated with carbogen (95% O_2 and 5% CO_2) to keep the pH within the physiologic range.

Primary cortical neurons were prepared from embryonic brains (E16-E18; C57BL/6). After isolating the anterior cortices, cells were separated by incubation with trypsin, DNAse, and mechanical dissociation. Neurons were plated on glass coverslips pre-coated with Poly-D-lysine hydrobromide (Sigma-Aldrich, Schnelldorf, Germany), and cultured in Neurobasal® medium (Life Technologies, Darmstadt, Germany) supplemented with 1 % glutamine, 1 % penicillin/streptomycin and 2 % supplement B-27. Cells were incubated at 37°C and 5 % CO_2 for 7 days before the experiments.

Labeling of mitochondria and experimental treatments

To label mitochondria, explanted ventral roots were incubated with 100 nM of MitoTracker® Orange (Life Technologies, Darmstadt, Germany) in oxygenated aCSF for 30 minutes at room temperature. Primary neurons were incubated with 100 nM of MitoTracker® Orange in Neurobasal® medium for 30 minutes at 37°C and 5 % CO_2. To measure mitochondrial membrane potential, ventral roots were incubated with 10 µg/ml of JC-1 (5,5',6,6'-tetrachloro-1,1',3,3'-tetraethylbenzimidazolyl-carbocyanine iodide; Life Technologies, Darmstadt, Germany) in oxygenated aCSF at room temperature for 1 hour.

For H_2O_2 treatment, explanted axons were incubated with 300 µM of H_2O_2 (Sigma-Aldrich, Schnelldorf, Germany) in aCSF with carbogen for 1 hour at room temperature. For NAD+ and methyl pyruvate treatment, (Sigma-Aldrich, Schnelldorf, Germany), axons were incubated with a mixture of 1 mM NAD+ and 20 mM methyl pyruvate, together with 300 µM hydrogen peroxide, in oxygenated aCSF at room temperature for 2 hours.

Mitochondrial imaging

Mitochondrial dynamics were imaged with an inverted laser-scanning confocal microscope adapted for live cell imaging (LSM 710, Carl Zeiss, Jena, Germany). MitoTracker Orange was excited with a DPSS laser at 561 nm, JC-1 was excited with dual illumination with argon (514 nm) and DPSS (561 nm) lasers, and CFP was excited with an argon laser at 405 nm. Mitochondria were visualized through a 100X/1.46 oil immersion objective (Plan-Apochromat, Carl Zeiss, Jena, Germany). Experiments with explanted roots were conducted at room temperature, and experiments with primary neurons were conducted at 37 °C and 5 % CO_2 (microscope incubator XL-3, Carl Zeiss, Jena, Germany). To image mitochondrial morphology, serial z stacks were acquired every 0.45 µm over 3.6 µm, with a resolution of 1024 x 1024 pixels. To image mitochondrial transport, 2D time-lapse images were acquired every 2 seconds over a total imaging time of 1 minute, with a resolution of 512 x 512 pixels.

To image mitochondrial internal structure, transected roots with or without H_2O_2 were fixed with 2 % glutaraldehyde and postfixed with 1 % OsO_4 and 0.8 % $K_4[Fe(CN)_6]$. 70-nm ultrathin sections were then cut, stained with uranyl acetate and lead citrate, and examined by transmission electron microscopy (EM 906, Carl Zeiss, Jena, Germany). These experiments were done in collaboration with the Institute of Vegetative Anatomy (Charité, Berlin).

Quantification of mitochondrial morphology and transport

To analyze mitochondrial shape, we used Volocity 6.0.1 (Perkin Elmer, Rodgau, Germany) and Image J 1.44 (NIH, USA, open source). Mitochondrial morphology was quantified by means of the

shape factor ($4\pi \times$ [Area]/[Perimeter]^2), a measure of circularity that ranges from 0 to 1, with 1 indicating a perfect circle.

Automated tracking of mitochondria was done with Volocity (v6.3, Perkin Elmer, Massachusetts, USA), Imaris (v7.6.4, Bitplane AG, Switzerland), wrMTrck (http://www.phage.dk/plugins/wrmtrck.html) and Difference Tracker (Andrews et al., 2010). To analyze the number of moving mitochondria, the number of tracks generated by each program were counted; only tracks with a displacement of at least 1 µm were considered motile. To establish the percentage of real tracks, the number of software-generated tracks that reproduced genuine mitochondrial trajectories were counted. Manual tracking of mitochondria was done with the Manual Tracking function of Volocity (v6.3), by clicking on the position of each mitochondrion in each time-lapse frame.

Idebenone treatment and detection

To examine the neuroprotective properties of idebenone *in vitro*, HT22 cells were incubated with various concentrations of idebenone in 1 % DMSO for 2 hours, followed by 5 mM or 10 mM glutamate (Sigma-Aldrich, Schnelldorf, Germany). To measure cell viability, cells were then stained with crystal violet and absorbance was read at 600 nm in a micro plate reader (Promega Glomax®, Mannheim, Germany; Herges et al., 2011).

To test the neuroprotective properties of idebenone *in vivo*, adult female C57BL/6 mice were immunized with 200 µg myelin oligodendrocyte glycoprotein (MOG)$_{35-55}$ peptide (purity > 95 %, Pepceuticals, Leicester, UK) in complete Freund's adjuvant to induce experimental autoimmune encephalomyelitis (EAE). Bordetella pertussis toxin (200 ng, PTX, List Biological Laboratories, Campbell, CA) was administered intra-peritoneally on the same day and 2 days after immunization to enhance the autoimmune response. They were weighed and scored daily as follows: 0 = no disease; 1 = tail paralysis; 2 = hindlimb paresis; 3 = hindlimb plegia; 4 = paraplegia and forelimb weakness; 5 = death due to EAE. 100 mg/kg idebenone (Santhera Pharmaceuticals, Switzerland) resuspended in 0.5 % carboxymethyl cellulose were then administered daily by oral gavage. Treatment was started either at day 7 after immunization (preventive treatment) or by reaching a clinical score of 1 (therapeutic treatment).

After terminating the experiments, brains and spinal cords were removed and stained with hematoxylin and eosin, luxol fast blue or Bielschowsky silver staining, according to standard protocols. Pictures were taken with a microscope Axio Observer.Z1 (Carl Zeiss, Jena, Germany) and a charge coupled device (CCD) camera (AxioCam ICc1, Carl Zeiss).

Penetration of idebenone in blood and cerebrospinal fluid was measured by liquid chromatography coupled to tandem mass spectrometry (LC–MS/MS) on a Kinetex C18 (Phenomenex, Aschaffenburg, Germany) and a 5500 QTrap® (AB Sciex, Darmstadt, Germany) controlled by Analyst® Software, version 1.5.1 (AB Sciex, Darmstadt, Germany). This was done in collaboration with the institute for Toxicology and Pharmacology (Labor Berlin).

Statistical analysis

Statistical analysis was performed using SPSS (IBM Deutschland, Ehningen, Germany) and Prism (Graph Pad, CA, USA). All data were evaluated for a Gaussian distribution with histograms and the Kolmogorov-Smirnov test. p-values below 0.05 were considered significant.

Results

1. Novel tools for studying mitochondrial dynamics in neurons

### 1.1 An *ex vivo* method for imaging mitochondrial transport

Explanted dorsal and ventral roots represent a simplified model system for imaging mitochondrial movements within axons. They contain peripheral sensory and motor axons, respectively, and preserved cellular interactions.

To obtain the explants, roots were cut at the exit point of the spinal cord, on one side, and before forming the spinal nerves, on the other (Fig. 1). The roots of the lower thoracic and lumbar regions were preferred, as they are longer than the cervical ones. Once transected, the roots were maintained in aCSF solution at room temperature, with continuous oxygenation and monitoring of the pH.
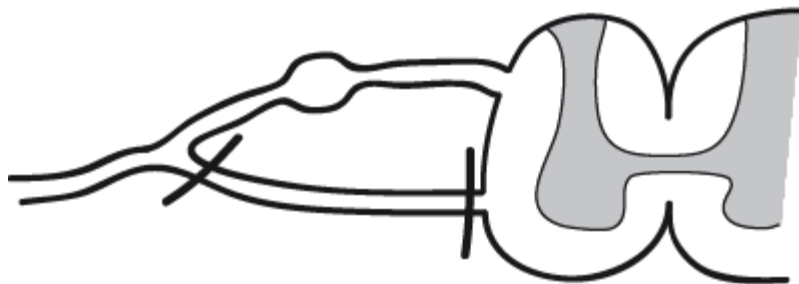
Fig. 1 Roots were explanted at the exit point of the spinal cord. Scheme of a spinal cord segment with the dorsal and the ventral root. The black lines show the segment of the ventral root that was typically sectioned.

In these axonal explants, about 15 % of mitochondria were mobile after axotomy. Mitochondrial transport remained stable for the first few hours after transection. Axonal mitochondria were easily labeled by incubating the axons with a membrane-permeant cationic mitochondrial dye, such as one of the MitoTracker probes (Life Technologies, Germany; Fig. 2). Alternatively, axons expressing a fluorescent protein specifically in the mitochondria were used without further labeling (e.g. strain B6.Cg-Tg(Thy1-CFP/COX8A)S2Lich/J, The Jackson Laboratory, Bar Harbor, Maine). If necessary, the mitochondrial membrane potential could be simultaneously assessed by co-labeling the mitochondria with a lipophilic potentiometric probe (e.g. TMRM or JC-1 dye; Bros et al., 2014).
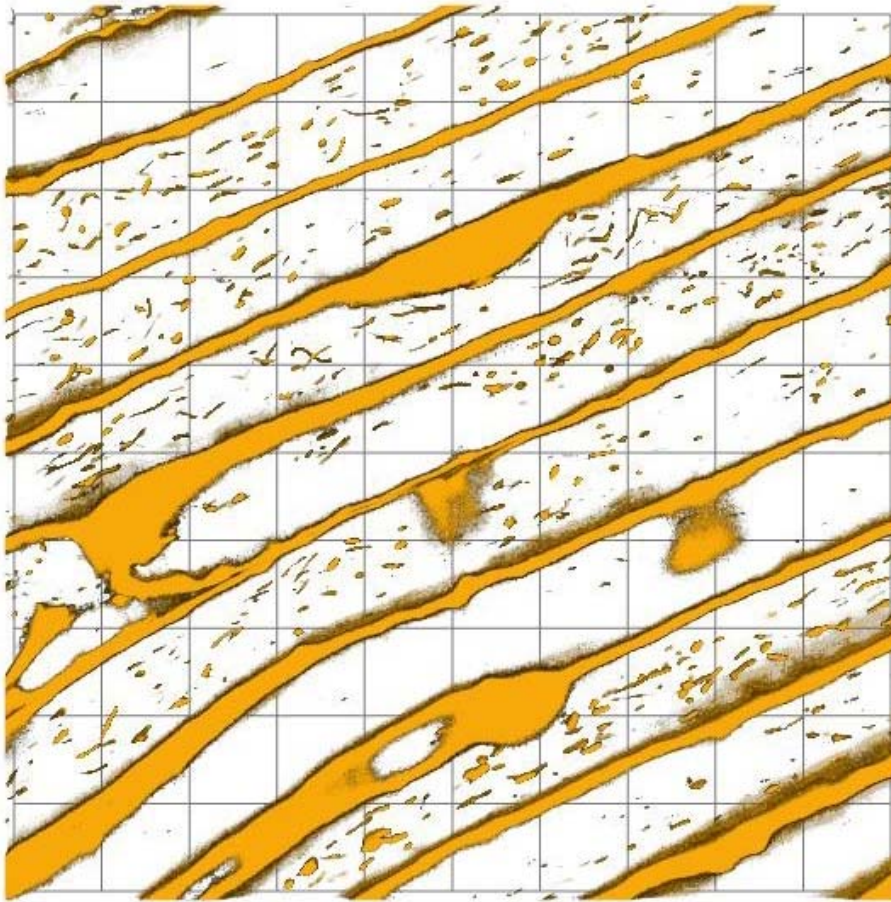
Fig. 2 Explanted roots were used to examine mitochondrial dynamics within axons. Confocal view of the interior of a transected ventral root stained with MitoTracker Orange, which labels both mitochondria and myelin. The axons are parallel and each of them contains several mitochondria. 1 unit: 10 μm.

Because the explanted roots were maintained in aqueous solution, the bathing medium could be modified to investigate how modulating ion channels or axonal homeostasis would affect mitochondrial behavior. This model was also used as a simplified platform for testing new therapeutic strategies targeting mitochondrial dynamics, thus avoiding problems resulting from poor penetration of the compound into the nervous system and low bioavailability. A step-by-step protocol on the explanting procedure, including troubleshooting, was published in Bros et al. (2015a).

1.2 Tools for tracking mitochondria within axons

Next, I investigated the suitability of various tracking methods for quantifying mitochondrial movements within axons. Mitochondria from explanted roots were labeled with MitoTracker Orange and tracked manually and with 4 programs for automated tracking: Volocity, Imaris, wrMTrck and Difference Tracker (DT; Fig. 3). The results from all strategies were then compared.
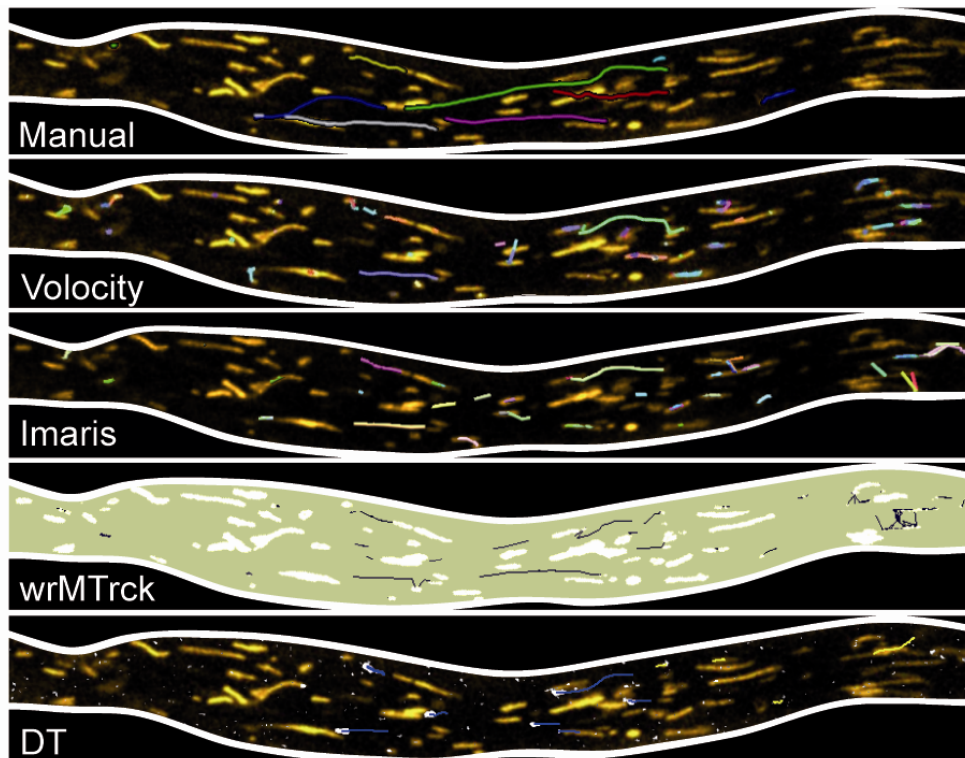
Fig. 3 Mitochondrial trajectories in an explanted ventral root obtained with manual and automated measurements. The colored lines represent the mitochondrial trajectories. In wrMTrck, the image was converted into binary; mitochondria were pseudocolored in white, mitochondrial trajectories in black and axonal cytoplasm in green. In DT, the moving particles are shown in white; the blue lines represent retrograde movements and the yellow lines represent anterograde movements. Modified from Bros et al., 2015b.

In general, profound differences between the manual and automated analysis were observed (Table 1). Track length (the total distance traveled by the mitochondria) was 54 - 67 % lower when measured automatically. Similarly, mitochondrial displacement (the shortest distance from the initial to the final position of the mitochondria) and track duration (the time during which a mitochondrion is in motion) were substantially underestimated by all automated tools. On the contrary, mitochondrial velocity was generally overestimated. Only the number of motile mitochondria and the directionality of the mitochondrial movements (anterograde vs. retrograde transport) were similar among methods. However, the Bland-Altman plots revealed a poor agreement between manual and automated strategies. The 95% limits of agreement were substantially wide in all 4 cases, reflecting considerable differences between the methods.

Furthermore, the automatically generated mitochondrial tracks did not always represent real mitochondrial movements. In fact, in explanted axons, less than 50 % of all generated tracks were true mitochondrial trajectories in 2 out of 4 tested applications.

The discrepancies between manual and automated tracking methods remained the same for both 2D and 3D data, and when mitochondrial transport was analyzed in cultured neurons. In addition to MitoTracker Orange staining, which only labels actively respiring mitochondria, mitochondrial motion was also analyzed in axons carrying a mitochondrially-targeted Cyan Fluorescent Protein (CFP) (Misgeld et al., 2007). The analysis outcome of CFP-labeled mitochondria was very similar to the results obtained with MitoTracker Orange, with a poor correlation and agreement between manual and automated strategies.

	Volocity	Imaris	wrMTrck	DT
Number of tracks	n.s.	n.s.	n.s.	n.s.
% of real tracks	52 (85.8)	38.2 (73.4)	27.1 (48.6)	75.3 (90.7)
Track length	↓↓↓	↓↓↓	↓↓↓	↓↓↓
Displacement	↓↓↓	↓↓↓	↓↓↓	↓↓↓
Track duration	↓↓↓	↓↓↓	↓↓↓	↓↓↓
Directionality	n.s.	n.s.	n.s.	n.s.
Velocity	n.s.	↑↑ (↑↑↑)	↑↑ (↑↑↑)	↑↑ (↑↑↑)

Table 1 Summary of the results produced by automated tracking tools compared with manual tracking. The values in brackets are from cultured neurons, and the other values are from explanted roots. n.s.: no statistical differences between manual and automated analysis; ↑↑: $p < 0.01$; ↑↑↑: $p < 0.001$. The direction of the arrow indicates whether the software produced higher (↑) or lower (↓) estimates compared with manual analysis (Bros et al., 2015b).

In view of the discrepancies between manual and automated methods, it was then investigated whether automated tools would at least be able to detect changes in mitochondrial transport caused by experimental interventions. For this purpose, explanted axons were treated with hydrogen peroxide (H_2O_2), which can reduce mitochondrial motility (Bros et al., 2014).

The manual analysis showed a significant reduction of mitochondrial motility in H_2O_2-treated axons compared with untreated controls. Consistently, all automated programs reported significantly reduced numbers of motile mitochondria (Fig. 4). Track length, mitochondrial displacement and velocity were similar between treated and untreated groups in both manual and most of the automated measurements.
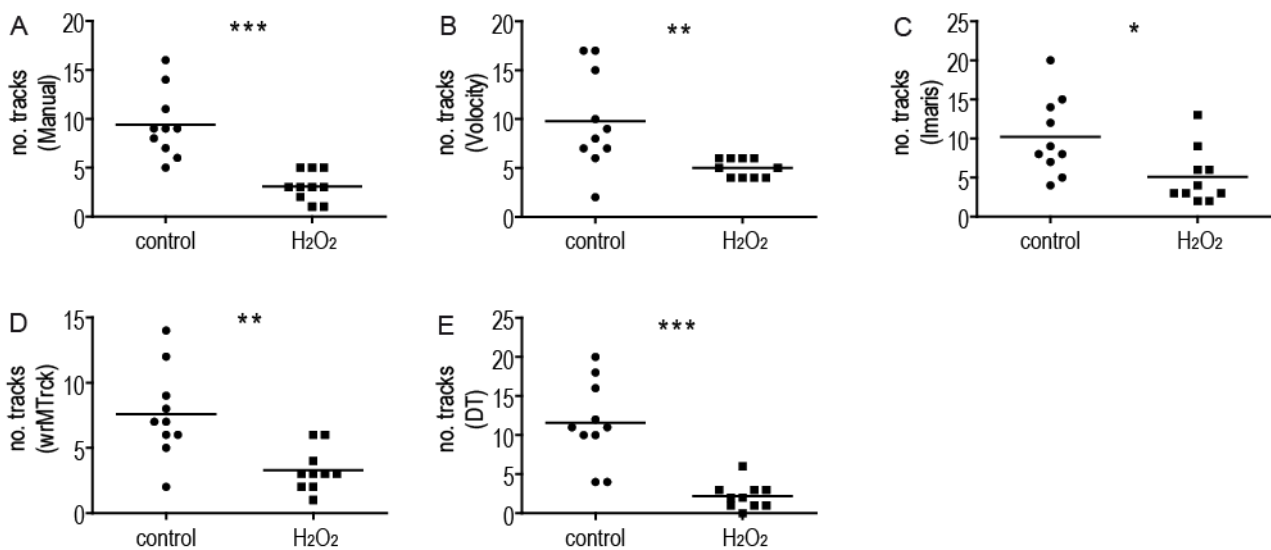
Fig. 4 Mitochondrial transport in untreated vs. H_2O_2-treated axons. Number of moving mitochondria obtained from manual analysis (A), Volocity (B), Imaris (C), wrMTrck (D) and DT (E) in untreated and H_2O_2-treated axons. n = 10 different axons; 40-100 mitochondria/axon. * $p < 0.05$, ** $p < 0.01$, *** $p < 0.001$. Modified from Bros et al., 2015b.

2. Initiation of mitochondrial damage following an oxidative insult

To explore whether oxidative stress could damage mitochondria within myelinated axons, ventral roots were exposed to 300 µM of H_2O_2 for 2 hours. Mitochondria became significantly shorter and rounder compared with unexposed controls (Fig. 5).
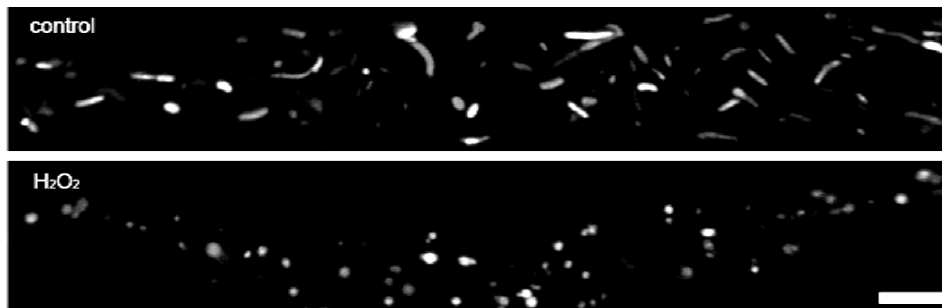
Fig. 5 Oxidative stress altered mitochondrial morphology within myelinated axons. Laser scanning confocal images of mitochondria within myelinated motor axons with (bottom) and without (top) H_2O_2. Scale bar: 5 µm. Modified from Bros et al., 2014.

However, this treatment did not affect all mitochondria at the same time. 30 minutes after applying H_2O_2, only mitochondria located proximal to the nodes of Ranvier had changed their morphology. Morphological alterations of internodal mitochondria were only visible after 120 minutes of incubation with H_2O_2 (Fig. 6,7A). Mitochondrial swellings began near the nodes of Ranvier and progressively extended to distal mitochondria on a bilateral manner.
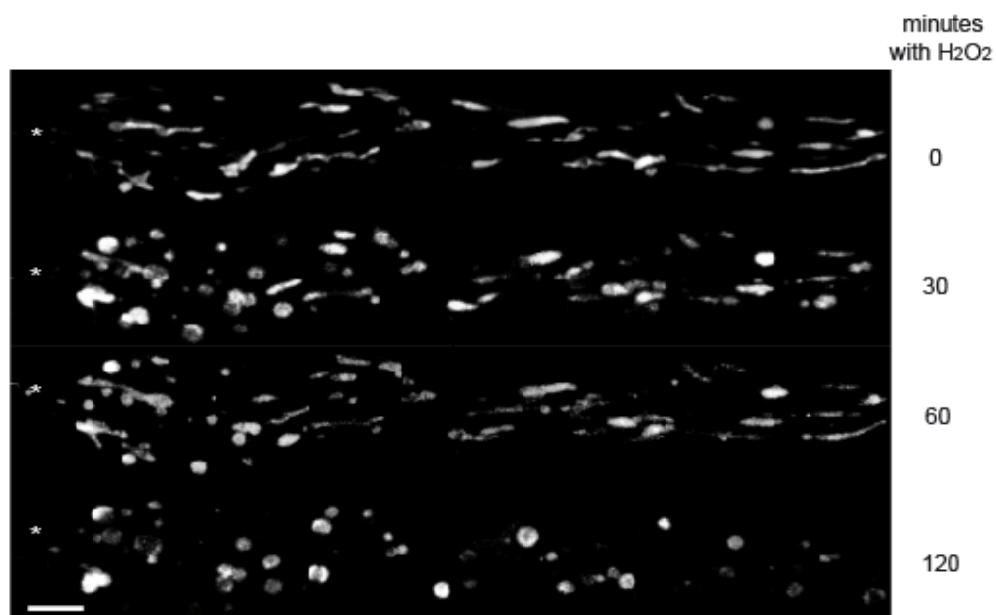
Fig. 6 Mitochondrial alterations initiated proximal to the nodes of Ranvier and progressed to the internodes. Mitochondria before (top) and 30, 60 and 120 minutes after applying H_2O_2. Nodes of Ranvier are located at the left side and are marked with an asterisk. Scale bar: 5 µm. Modified from Bros et al., 2014.

With electron microscopy it was confirmed that, in addition to an abnormal external morphology, nodal mitochondria had collapsed cristae. In contrast, the internal structure of internodal mitochondria was preserved (Fig. 7B). Therefore, it was then investigated whether exposure to H_2O_2 affected also the mitochondrial membrane potential. This was done by labeling the mitochondria with the potentiometric indicator JC-1, whose emitted fluorescence shifts from red (590 nm) to green (529 nm) upon depolarization. Indeed, H_2O_2 induced mitochondrial depolarization, which also initiated near the nodes of Ranvier. Accordingly, MitoTracker Orange diffusion—which correlated with JC-1 depolarization—was most intense in the nodal proximities, compared with the internodes (Fig. 7C).

Next, it was examined whether oxidative stress would interfere with mitochondrial trafficking in the axons, and whether this would also initiate at the nodes of Ranvier. To quantify mitochondrial transport, 10-µm-long axonal segments from the nodes and the internodes were selected, and the number of mitochondria moving over 1 minute counted. Mitochondria were considered motile when their displacement was ≥ 1 µm. Mitochondrial transport at the nodes of Ranvier in H_2O_2-treated axons was significantly lower than in controls. In the internodes, however, both groups presented a similar number of moving mitochondria, suggesting that the transport was interrupted initially at the nodes of Ranvier (Fig. 7D).
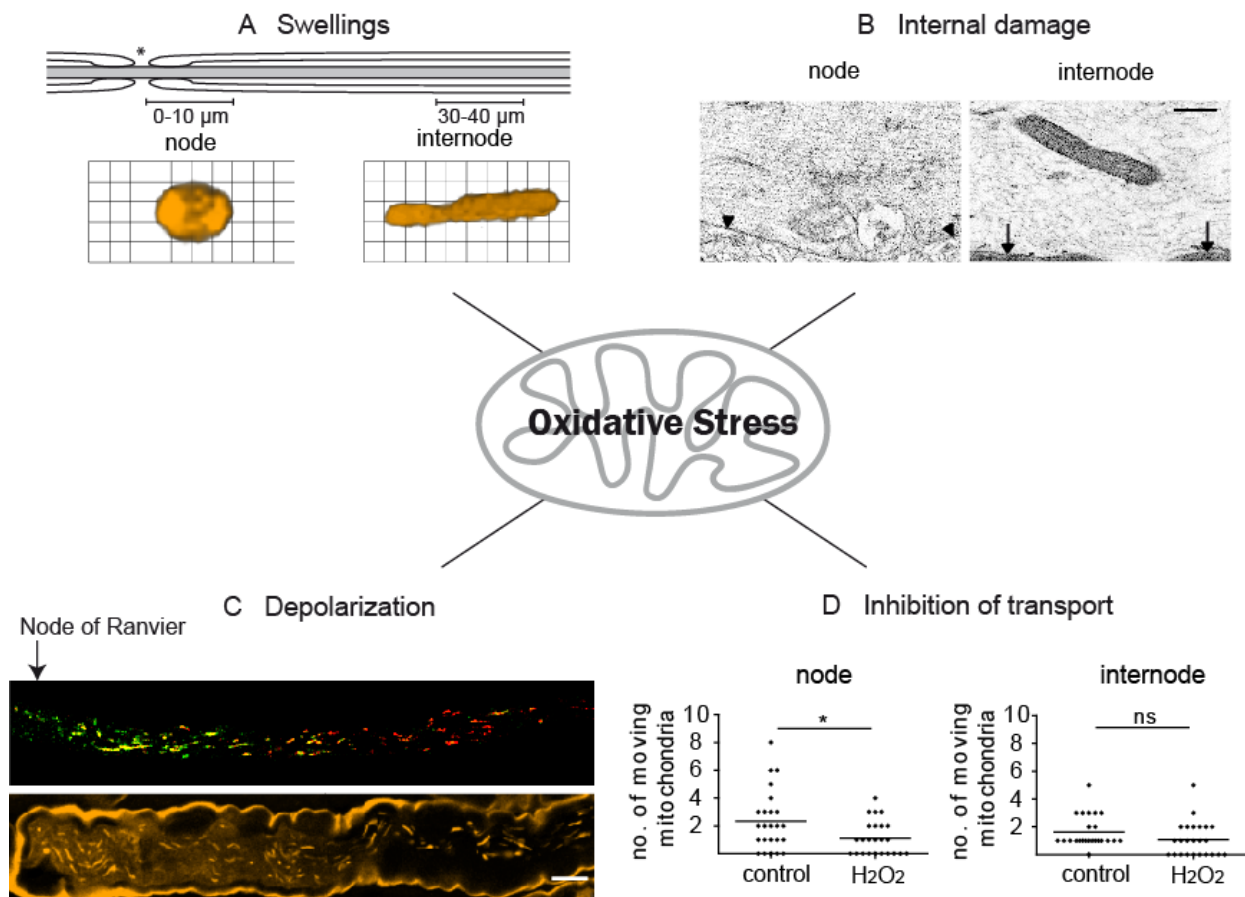
Fig. 7 Following an oxidative insult, mitochondrial swellings, damage to the cristae, depolarization and inhibition of axonal transport initiated near the nodes of Ranvier. A. 3D reconstructions of nodal and internodal mitochondria labeled with MitoTracker Orange. 1 unit: 0.4 µm. B. Electron micrographs of nodal and internodal mitochondria. The arrows point at the myelin sheath, and the arrowheads delineate the node of Ranvier, without myelin. 12930 X. Scale bar: 0.5 µm. C. JC-1 (top) and MitoTracker Orange (bottom) staining of H_2O_2-treated axons. Scale bar: 5 µm. D. Motility of mitochondria at the nodes of Ranvier and at the internodes. N = 24 axons. Modified from Bros et al., 2014.

We then investigated whether oxidative damage to mitochondria could be prevented pharmacologically. For this purpose, a combination of nicotinamide adenine dinucleotide (NAD+) and pyruvate (both needed to generate ATP via the oxidative phosphorylation pathway) was used, as these had been shown to delay axon degeneration in both transected sciatic nerves (Park et al., 2013) and cultured dorsal root ganglia explants (Wang et al., 2005). After 2 hours of incubation with H_2O_2, both nodal and internodal mitochondria were clearly altered (Fig. 8A). However, supplementation of NAD+ and methyl pyruvate rendered mitochondria resistant to oxidative changes (Fig. 8B): While 72% of axons contained spherical mitochondria when incubated with H_2O_2, only 17% of axons contained abnormal mitochondria when co-incubated with NAD+ and methyl pyruvate. NAD+ and methyl pyruvate protected mitochondria equally within the two heminodes. Moreover, NAD+ and methyl pyruvate prevented mitochondrial depolarization following H_2O_2 exposure (Bros et al., 2014).

Finally, it was examined whether preventing oxidative damage to mitochondria would also protect axons from degeneration. Transected axons were incubated with H_2O_2 for 8 hours, until several axons had developed swellings and spheroids and mitochondria were depolarized (Fig. 8C). When NAD+ and methyl pyruvate were included in the extracellular solution, no morphological signs of axon degeneration were detected (Fig. 8D). Moreover, mitochondria were actively respiring and energized. Most of them were elongated, even proximal to the nodes of Ranvier. Thus, NAD+ and pyruvate not only protected mitochondria from oxidative damage, but also prevented subsequent degeneration of axons.
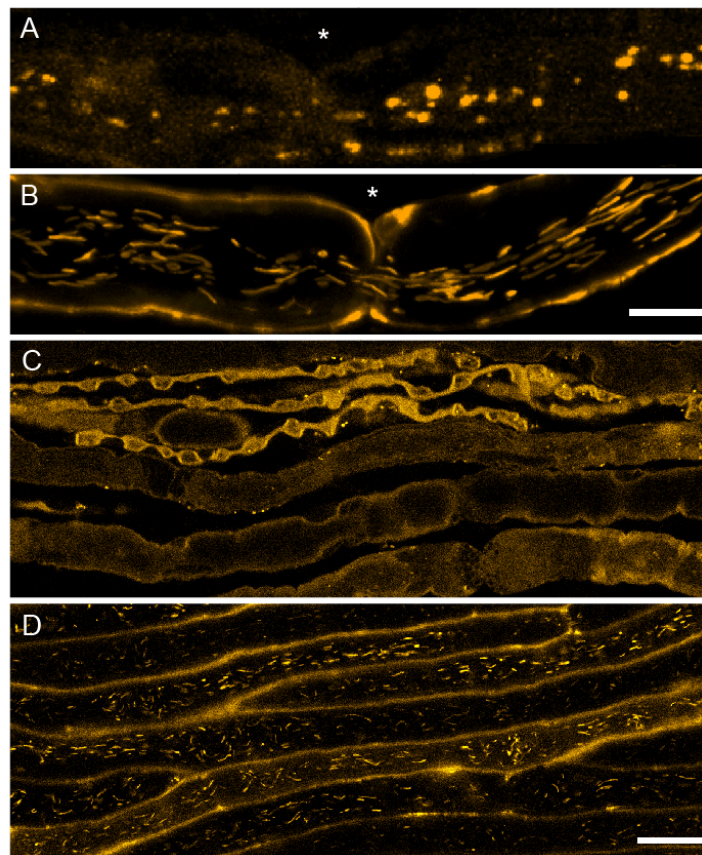
Fig. 8 NAD+ and pyruvate protected mitochondria from oxidative damage and prevented axonal degeneration. Axon incubated for 2 hours only with H_2O_2 (A) or with NAD+ and methyl pyruvate in addition to H_2O_2 (B). The nodes of Ranvier are marked with an asterisk. Scale bar: 10 μm. Transected axons incubated for 8 hours only with H_2O_2 (C) or with H_2O_2, NAD+ and methyl pyruvate (D). Scale bar: 20 μm. Modified from Bros et al., 2014.

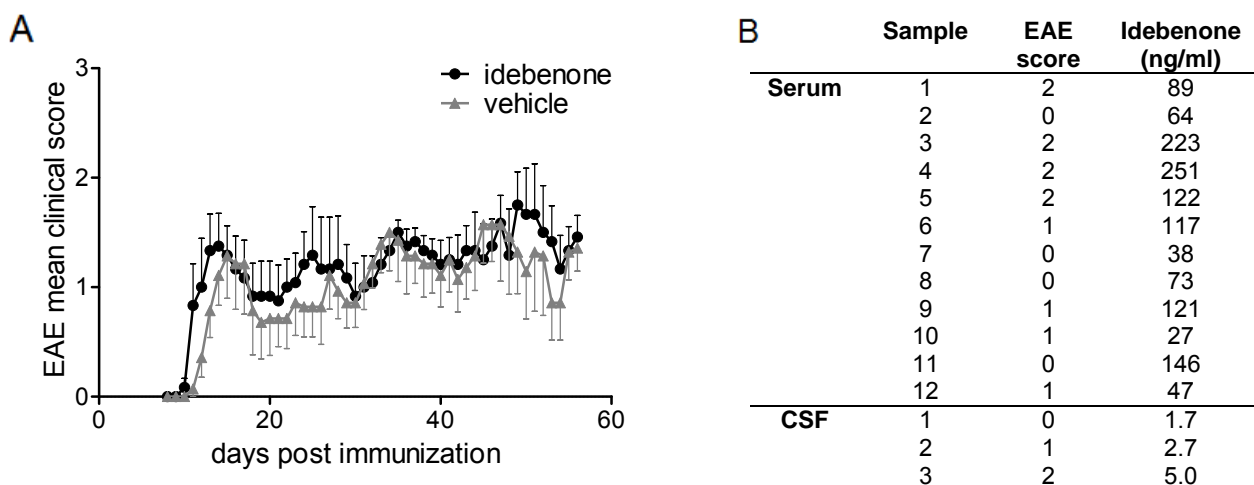## 3. Antioxidant therapy in a model of chronic CNS inflammation

Because oxidative stress plays a critical role in mitochondrial and axonal damage, it was investigated whether the antioxidant idebenone, a synthetic derivative of co-enzyme Q10, was neuroprotective *in vitro*, in a neuronal cell line, and *in vivo*, in chronic EAE.

Murine hippocampal HT22 cells were first pre-incubated with 0, 1, 5, or 10 μM idebenone for 2 hours. To induce cell death, cells were then incubated with either 5 mM or 10 mM glutamate. In agreement with a previous report (Miyamoto et al., 1989), idebenone protected the cells against cell death induced by both 5 and 10 mM glutamate in a dose dependent manner.

Given these neuroprotective results, the therapeutic potential of idebenone was then investigated in the EAE model. Idebenone was applied following two different treatment strategies: a preventative regime (i.e. starting on day 7 after immunization) and a therapeutic regime (i.e. with the first signs of disability, represented by a score of 1). Idebenone or vehicle control was administered by oral gavage once daily. The preventative treatment did not affect EAE incidence or delay the time of disease onset (Fig. 9A). Moreover, neither treatment affected the clinical severity of the disease, or had any effect on the cumulative disease activity.

Idebenone also did not show any subclinical effects on inflammation, demyelination or axonal injury in the CNS, as shown by H&E, LFB and Bielschowsky silver staining, respectively, on transverse spinal cord sections.

In view of the lack of clinical effects, we then verified that orally-administered idebenone entered the circulation and penetrated the CNS. Blood and cerebrospinal fluid (CSF) samples were collected for determination of the drug concentration by liquid chromatography coupled with mass spectrometry (LC–MS/MS). This analysis confirmed that idebenone was able to penetrate into both blood and CNS. Moreover, those cases that showed higher EAE severity correlated with a greater penetration of idebenone into the CSF, which might be the result of a greater disruption of the blood–brain-barrier (Fig. 9B).

	Sample	EAE score	Idebenone (ng/ml)
Serum	1	2	89
	2	0	64
	3	2	223
	4	2	251
	5	2	122
	6	1	117
	7	0	38
	8	0	73
	9	1	121
	10	1	27
	11	0	146
	12	1	47
CSF	1	0	1.7
	2	1	2.7
	3	2	5.0

Fig. 9 Idebenone penetrated into blood and CNS but did not affect EAE clinical course. A. Mean clinical scores after oral treatment with idebenone or vehicle in a preventative regime (mean ± SEM). B. EAE score and idebenone concentrations in serum and CSF. Modified (Fiebiger et al., 2013).

Discussion

Oxidative stress and mitochondrial dysfunction contribute to the progression of neurodegenerative disorders. However, how these two processes interact to cause axonal and neuronal damage remains unknown. In this series of studies, I first established methods for visualizing and quantifying axonal mitochondrial dynamics in axons, and then investigated how oxidative stress alters axonal mitochondria and contributes to axonal degeneration.

Mitochondrial dynamics in explanted roots resemble those of the non-transected axons, and were therefore used as a simplified model system for monitoring mitochondrial behavior. In the axons from explanted roots, about 15 % of mitochondria were motile within the first hours after axotomy, which is consistent with data on entire neurons (Misgeld et al., 2007). Moreover, mitochondria maintained an elongated morphology, similar to that observed *in vivo* (Misgeld et al., 2007).

Explanted roots offer a number of unique advantages over other methods traditionally used to investigate mitochondrial transport:

- They combine a preserved tissue cytoarchitecture and cellular interactions with the simplicity of *in vitro* preparations. The entire explanting procedure takes less than 30 minutes.

- Mitochondrial dynamics can be studied specifically in either sensory or motor axons, by explanting dorsal or ventral roots, respectively.

- The somata, dendrites and synaptic terminals are not included in the preparation. Mitochondria can be exclusively analyzed in the axons.

- Peripheral axons from spinal roots are thicker than axons from dissociated CNS cells. They also have a higher mitochondrial density, so that more objects can be simultaneously examined.

- As opposed to more complex systems, such as brain slices or *in vivo* intravital imaging, axonal mitochondria are easily identified and differentiated from mitochondria of other cell populations without additional markers. Similarly, due to the parallel organization of the axons, mitochondria pertaining to the same axon are easily recognized.

- A fraction of axons are running superficially (within the first 20 µm). It is not necessary to image deep into the tissue, thus limiting scattering of light.

- Alterations of mitochondrial dynamics are not triggered by signals from the cell body, nor are they influenced by the immune system. The effect of cell body signaling pathways or inflammatory mediators can be separately examined.

- Axons can be explanted independently of the age and genetic background, which might be useful for investigating mitochondrial dynamics in experimental disease models.

Nevertheless, a limitation of this model is that mitochondrial transport begins to decrease a few hours after axon transection, which might prevent investigations with neuroprotective or neurotoxic compounds with longer action mechanisms. The timing of the experiments in relation to axotomy has to be strictly controlled.

Axonal mitochondria can then be tracked manually, by clicking on the position of each mitochondrion over time. However, this can be extremely time-consuming and introduce measurement error. Moreover, it is not feasible in models where mitochondria do not follow a straight trajectory, such in cell bodies. I therefore determined whether automated programs for particle tracking, in which mitochondria are detected and linked without the continuous input of the operator, can substitute manual analysis. For this, mitochondria were tracked with 4 automated programs, and the results were compared to those obtained manually.

The correlation and agreement between manual and automated methods was poor. This was most pronounced when length of mitochondrial trajectories, mitochondrial displacement and duration of movement were assessed—with reductions of up to 77 % compared to the manual values. Despite these negative results, all automated applications were able to detect a decrease in mitochondrial transport in H_2O_2-treated axons, compared with untreated controls. Thus, although these results do not support the use of automated and manual tools interchangeably for absolute quantification of mitochondrial dynamics, automated tools might be suitable to assess differences in mitochondrial transport between experimental groups.

Next, by using explanted ventral roots, I showed that oxidative stress altered mitochondrial dynamics and function in myelinated axons. Mitochondria underwent a number of changes following the oxidative insult: they became depolarized, the mitochondrial cristae unfolded and the axonal transport was reduced. Mitochondria lost their elongated morphology and became shorter and rounder. All this happened before any detectable signs of axonal degeneration. In agreement with these data, other studies showed mitochondrial changes preceding axon degeneration, suggesting that mitochondrial dysfunction is an early event that can be targeted to prevent subsequent axonal damage (Jaarsma et al., 2001; Qi et al., 2006; Nikic et al., 2011; Vande Velde et al., 2011).

This is important because in MS, activated immune cells in the CNS produce vast amounts of oxygen free radicals (Glass et al., 2010). Demyelinated axons, which lack trophic support from the myelin and are directly exposed to the extracellular environment, are more vulnerable to oxidative stress (Trapp and Nave, 2008; Trapp and Stys, 2009). In agreement with this, it was shown here that oxidative damage to mitochondria initiates at the nodes of Ranvier, the small unmyelinated segments in the axon.

Apart from lacking myelin, the nodes of Ranvier concentrate the highest density of voltage-gated sodium channels in the axon. Previous investigations in unmyelinated neurons showed that oxidative stress induces Na^+ influxes into the axon (Barsukova et al., 2012). Therefore, in myelinated axons, oxidative stress-induced entry of Na^+ might be localized at the nodes of Ranvier. The ATP-dependent Na^+/K^+ pump keeps intraaxonal Na^+ concentration low. However, when the energetic supply is limited (e.g. due to mitochondrial damage) or when there is an excess of Na^+ flow into the axon (e.g. during oxidative stress caused by sustained inflammation), Na^+ can be exchanged by Ca^{2+} (Craner et al., 2004). Intraaxonal Ca^{2+} can then activate the mitochondrial permeability transition pore (mPTP) of the inner mitochondrial membrane, with detrimental effects

for the cell. Indeed, all mitochondrial changes observed here are consistent with an activation of the mPTP (Rasola and Bernardi, 2007).

To confirm that dysregulation of axonal bioenergetics is involved in mitochondrial damage, axons were treated with NAD+ and pyruvate, which have been shown to prevent the decrease of ATP in injured axons (Wang et al., 2005; Park et al., 2013). Indeed, by applying these mitochondrial substrates together with an oxidative insult, mitochondria became resistant to oxidative-stress induced changes and axons were protected against degeneration.

Next, it was investigated whether the antioxidant idebenone, a synthetic analog of coenzyme Q_{10} that has proven beneficial in Friedreich's ataxia (Di Prospero et al., 2007) and Leber's hereditary optic neuropathy (Heitz et al., 2012), would also have neuroprotective effects in EAE resulting in a better disease outcome. Although idebenone protected neuronal cells *in vitro*, neither a preventive (starting before disease onset) nor a therapeutic regimen (starting with the first signs of disability) had any effect on disease development or severity *in vivo*.

Insufficient dosage of idebenone was likely not the cause of negative effects, as the same dose of the compound had proven beneficial in other models of neurological disorders (Nagaoka et al., 1989; Scavini et al., 1996; Grieb et al., 1998). Additionally, using LC–MS/MS it was verified that the drug entered the circulation and reached the CSF.

Although idebenone had been shown to decrease oxidative stress *in vivo* (Nagaoka et al., 1989; Ahmed, 2014), it cannot be concluded from the present experiments that oxidative stress had been actually reduced after the treatment, as the study lacked validated biomarkers of oxidative stress in the CNS. Alternatively, the lack of neuroprotection might have been due to an inappropriate or excessive ROS reduction, as it might have interfered with the physiological ROS signaling in the cell, and the resulting side effects masked the potential beneficial actions of idebenone (Saso and Firuzi, 2014).

Moreover, the antioxidant effect of idebenone might have been insufficient on its own to show clinical efficacy in this disease. As suggested by Saso and Firuzi (2014), a combination of more than one antioxidant or of an antioxidant with another drug might be needed to adequately control oxidative damage. Both MS and EAE are complex pathologies with intricate interactions between the immune and the nervous system, and oxidative stress might be only one of several mechanisms contributing to axonal damage. Combination therapies targeting multiple pathogenic aspects have already shown promise for MS (Conway and Cohen, 2010; Herges et al., 2011; Reick et al., 2014).

In conclusion, these experiments provide methodological advances for monitoring and quantifying mitochondrial transport in axons. *Ex vivo* transected roots are a suitable model for examining the influence of various pathogenic conditions and therapeutic strategies on axonal and mitochondrial damage. However, quantification of mitochondrial transport is complex, and algorithms for automated mitochondrial tracking need to be refined to be able to substitute manual tracking. Until then, automated tools should be limited to comparisons of differences between experimental groups. By using these methods, I then demonstrated that the nodes of Ranvier are a key location for the initiation of mitochondrial damage by oxidative stress, which can occur in the absence of

demyelination and promote axonal death. Despite a critical role of oxidative stress in mitochondrial damage, the antioxidant idebenone did not show any beneficial effects in a model of chronic neuroinflammation. I propose that the unique ionic specializations and high energy requirements at the nodes of Ranvier make them a vulnerable axonal location that leads to early mitochondrial damage, and might thus constitute an effective therapeutic target for chronic neuroinflammatory diseases with a degenerative component.

References

Ahmed MA (2014) Neuroprotective effects of idebenone against pilocarpine-induced seizures: modulation of antioxidant status, DNA damage and Na(+), K (+)-ATPase activity in rat hippocampus. Neurochem Res 39:394-402.

Andrews S, Gilley J, Coleman MP (2010) Difference Tracker: ImageJ plugins for fully automated analysis of multiple axonal transport parameters. J Neurosci Methods 193:281-287.

Barsukova AG, Forte M, Bourdette D (2012) Focal increases of axoplasmic Ca2+, aggregation of sodium-calcium exchanger, N-type Ca2+ channel, and actin define the sites of spheroids in axons undergoing oxidative stress. J Neurosci 32:12028-12037.

Bros H, Niesner R, Infante-Duarte C (2015a) An ex vivo model for studying mitochondrial trafficking in neurons. Methods Mol Biol 1264:465-472.

Bros H, Millward JM, Paul F, Niesner R, Infante-Duarte C (2014) Oxidative damage to mitochondria at the nodes of Ranvier precedes axon degeneration in ex vivo transected axons. Exp Neurol 261C:127-135.

Bros H, Hauser A, Paul F, Niesner R, Infante-Duarte C (2015b) Assessing mitochondrial movement within neurons: manual vs. automated tracking methods. Traffic.

Campbell GR, Worrall JT, Mahad DJ (2014) The central role of mitochondria in axonal degeneration in multiple sclerosis. Mult Scler 20:1806-1813.

Chang DT, Reynolds IJ (2006) Mitochondrial trafficking and morphology in healthy and injured neurons. Prog Neurobiol 80:241-268.

Chang DT, Rintoul GL, Pandipati S, Reynolds IJ (2006) Mutant huntingtin aggregates impair mitochondrial movement and trafficking in cortical neurons. Neurobiol Dis 22:388-400.

Conway D, Cohen JA (2010) Combination therapy in multiple sclerosis. Lancet Neurol 9:299-308.

Craner MJ, Newcombe J, Black JA, Hartle C, Cuzner ML, Waxman SG (2004) Molecular changes in neurons in multiple sclerosis: altered axonal expression of Nav1.2 and Nav1.6 sodium channels and Na+/Ca2+ exchanger. Proc Natl Acad Sci U S A 101:8168-8173.

De Vos KJ, Chapman AL, Tennant ME, Manser C, Tudor EL, Lau KF, Brownlees J, Ackerley S, Shaw PJ, McLoughlin DM, Shaw CE, Leigh PN, Miller CC, Grierson AJ (2007) Familial amyotrophic lateral sclerosis-linked SOD1 mutants perturb fast axonal transport to reduce axonal mitochondria content. Hum Mol Genet 16:2720-2728.

Di Prospero NA, Baker A, Jeffries N, Fischbeck KH (2007) Neurological effects of high-dose idebenone in patients with Friedreich's ataxia: a randomised, placebo-controlled trial. Lancet Neurol 6:878-886.

Fang C, Bourdette D, Banker G (2012) Oxidative stress inhibits axonal transport: implications for neurodegenerative diseases. Mol Neurodegener 7:29.

Fiebiger SM, Bros H, Grobosch T, Janssen A, Chanvillard C, Paul F, Dorr J, Millward JM, Infante-Duarte C (2013) The antioxidant idebenone fails to prevent or attenuate chronic experimental autoimmune encephalomyelitis in the mouse. J Neuroimmunol 262:66-71.

Friese MA, Schattling B, Fugger L (2014) Mechanisms of neurodegeneration and axonal dysfunction in multiple sclerosis. Nat Rev Neurol 10:225-238.

Glass CK, Saijo K, Winner B, Marchetto MC, Gage FH (2010) Mechanisms underlying inflammation in neurodegeneration. Cell 140:918-934.

Grieb P, Ryba MS, Debicki GS, Gordon-Krajcer W, Januszewski S, Chrapusta SJ (1998) Changes in oxidative stress in the rat brain during post-cardiac arrest reperfusion, and the effect of treatment with the free radical scavenger idebenone. Resuscitation 39:107-113.

Harding AE, Sweeney MG, Miller DH, Mumford CJ, Kellar-Wood H, Menard D, McDonald WI, Compston DA (1992) Occurrence of a multiple sclerosis-like illness in women who have a Leber's hereditary optic neuropathy mitochondrial DNA mutation. Brain 115 (Pt 4):979-989.

Heitz FD, Erb M, Anklin C, Robay D, Pernet V, Gueven N (2012) Idebenone protects against retinal damage and loss of vision in a mouse model of Leber's hereditary optic neuropathy. PLoS One 7:e45182.

Herges K, Millward JM, Hentschel N, Infante-Duarte C, Aktas O, Zipp F (2011) Neuroprotective effect of combination therapy of glatiramer acetate and epigallocatechin-3-gallate in neuroinflammation. PLoS One 6:e25456.

Horvath R, Abicht A, Shoubridge EA, Karcagi V, Rozsa C, Komoly S, Lochmuller H (2000) Leber's hereditary optic neuropathy presenting as multiple sclerosis-like disease of the CNS. J Neurol 247:65-67.

Jaarsma D, Rognoni F, van Duijn W, Verspaget HW, Haasdijk ED, Holstege JC (2001) CuZn superoxide dismutase (SOD1) accumulates in vacuolated mitochondria in transgenic mice expressing amyotrophic lateral sclerosis-linked SOD1 mutations. Acta Neuropathol 102:293-305.

Jansen PH, van der Knaap MS, de Coo IF (1996) Leber's hereditary optic neuropathy with the 11 778 mtDNA mutation and white matter disease resembling multiple sclerosis: clinical, MRI and MRS findings. J Neurol Sci 135:176-180.

Lassmann H, van Horssen J, Mahad D (2012) Progressive multiple sclerosis: pathology and pathogenesis. Nat Rev Neurol 8:647-656.

Lin MT, Beal MF (2006) Mitochondrial dysfunction and oxidative stress in neurodegenerative diseases. Nature 443:787-795.

Lublin FD, Reingold SC (1996) Defining the clinical course of multiple sclerosis: results of an international survey. National Multiple Sclerosis Society (USA) Advisory Committee on Clinical Trials of New Agents in Multiple Sclerosis. Neurology 46:907-911.

Lucchinetti C, Bruck W, Parisi J, Scheithauer B, Rodriguez M, Lassmann H (2000) Heterogeneity of multiple sclerosis lesions: implications for the pathogenesis of demyelination. Ann Neurol 47:707-717.

Mahad D, Ziabreva I, Lassmann H, Turnbull D (2008) Mitochondrial defects in acute multiple sclerosis lesions. Brain 131:1722-1735.

Mahad DJ, Ziabreva I, Campbell G, Lax N, White K, Hanson PS, Lassmann H, Turnbull DM (2009) Mitochondrial changes within axons in multiple sclerosis. Brain 132:1161-1174.

Misgeld T, Kerschensteiner M, Bareyre FM, Burgess RW, Lichtman JW (2007) Imaging axonal transport of mitochondria in vivo. Nat Methods 4:559-561.

Miyamoto M, Murphy TH, Schnaar RL, Coyle JT (1989) Antioxidants protect against glutamate-induced cytotoxicity in a neuronal cell line. J Pharmacol Exp Ther 250:1132-1140.

Nagaoka A, Suno M, Shibota M, Kakihana M (1989) Effects of idebenone on neurological deficits, local cerebral blood flow, and energy metabolism in rats with experimental cerebral ischemia. Arch Gerontol Geriatr 8:193-202.

Nikic I, Merkler D, Sorbara C, Brinkoetter M, Kreutzfeldt M, Bareyre FM, Bruck W, Bishop D, Misgeld T, Kerschensteiner M (2011) A reversible form of axon damage in experimental autoimmune encephalomyelitis and multiple sclerosis. Nat Med 17:495-499.

Park JY, Jang SY, Shin YK, Koh H, Suh DJ, Shinji T, Araki T, Park HT (2013) Mitochondrial swelling and microtubule depolymerization are associated with energy depletion in axon degeneration. Neuroscience 238:258-269.

Qi X, Lewin AS, Sun L, Hauswirth WW, Guy J (2006) Mitochondrial protein nitration primes neurodegeneration in experimental autoimmune encephalomyelitis. J Biol Chem 281:31950-31962.

Rasola A, Bernardi P (2007) The mitochondrial permeability transition pore and its involvement in cell death and in disease pathogenesis. Apoptosis 12:815-833.

Reick C, Ellrichmann G, Thone J, Scannevin RH, Saft C, Linker RA, Gold R (2014) Neuroprotective dimethyl fumarate synergizes with immunomodulatory interferon beta to provide enhanced axon protection in autoimmune neuroinflammation. Exp Neurol 257:50-56.

Saso L, Firuzi O (2014) Pharmacological applications of antioxidants: lights and shadows. Curr Drug Targets 15:1177-1199.

Sawcer S et al. (2011) Genetic risk and a primary role for cell-mediated immune mechanisms in multiple sclerosis. Nature 476:214-219.

Saxton WM, Hollenbeck PJ (2012) The axonal transport of mitochondria. J Cell Sci 125:2095-2104.

Scalfari A, Neuhaus A, Degenhardt A, Rice GP, Muraro PA, Daumer M, Ebers GC (2010) The natural history of multiple sclerosis: a geographically based study 10: relapses and long-term disability. Brain 133:1914-1929.

Scavini C, Rozza A, Lanza E, Favalli L, Racagni G, Brunello N (1996) Effect of idebenone on in vivo serotonin release and serotonergic receptors in young and aged rats. Eur Neuropsychopharmacol 6:95-102.

Schon EA, Przedborski S (2011) Mitochondria: the next (neurode)generation. Neuron 70:1033-1053.

Sheng ZH, Cai Q (2012) Mitochondrial transport in neurons: impact on synaptic homeostasis and neurodegeneration. Nat Rev Neurosci 13:77-93.

Stokin GB, Lillo C, Falzone TL, Brusch RG, Rockenstein E, Mount SL, Raman R, Davies P, Masliah E, Williams DS, Goldstein LS (2005) Axonopathy and transport deficits early in the pathogenesis of Alzheimer's disease. Science 307:1282-1288.

Trapp BD, Nave KA (2008) Multiple sclerosis: an immune or neurodegenerative disorder? Annu Rev Neurosci 31:247-269.

Trapp BD, Stys PK (2009) Virtual hypoxia and chronic necrosis of demyelinated axons in multiple sclerosis. Lancet Neurol 8:280-291.

Trapp BD, Peterson J, Ransohoff RM, Rudick R, Mork S, Bo L (1998) Axonal transection in the lesions of multiple sclerosis. N Engl J Med 338:278-285.

Trushina E et al. (2004) Mutant huntingtin impairs axonal trafficking in mammalian neurons in vivo and in vitro. Mol Cell Biol 24:8195-8209.

Vande Velde C, McDonald KK, Boukhedimi Y, McAlonis-Downes M, Lobsiger CS, Bel Hadj S, Zandona A, Julien JP, Shah SB, Cleveland DW (2011) Misfolded SOD1 associated with motor neuron mitochondria alters mitochondrial shape and distribution prior to clinical onset. PLoS One 6:e22031.

Wang J, Zhai Q, Chen Y, Lin E, Gu W, McBurney MW, He Z (2005) A local mechanism mediates NAD-dependent protection of axon degeneration. J Cell Biol 170:349-355.

Wingerchuk DM, Carter JL (2014) Multiple sclerosis: current and emerging disease-modifying therapies and treatment strategies. Mayo Clin Proc 89:225-240.

Witte ME, Bo L, Rodenburg RJ, Belien JA, Musters R, Hazes T, Wintjes LT, Smeitink JA, Geurts JJ, De Vries HE, van der Valk P, van Horssen J (2009) Enhanced number and activity of mitochondria in multiple sclerosis lesions. J Pathol 219:193-204.

EIDESSTATTLICHE VERSICHERUNG

(affidavit)

Ich, Elena Bros, versichere an Eides statt durch meine eigenhändige Unterschrift, dass ich die vorgelegte Dissertation mit dem Thema: „Mitochondrial damage and axon degeneration in chronic neuroinflammation" selbstständig und ohne nicht offengelegte Hilfe Dritter verfasst und keine anderen als die angegebenen Quellen und Hilfsmittel genutzt habe.

Alle Stellen, die wörtlich oder dem Sinne nach auf Publikationen oder Vorträgen anderer Autoren beruhen, sind als solche in korrekter Zitierung (siehe „Uniform Requirements for Manuscripts, URM" des ICMJE, www.**icmje**.org) kenntlich gemacht. Die Abschnitte zu Methodik (insbesondere praktische Arbeiten, Laborbestimmungen, statistische Aufarbeitung) und Resultaten (insbesondere Abbildungen, Graphiken und Tabellen) entsprechen den URM und werden von mir verantwortet.

Meine Anteile an den ausgewählten Publikationen entsprechen denen, die in der untenstehenden gemeinsamen Erklärung mit der Betreuerin, angegeben sind. Sämtliche Publikationen, die aus dieser Dissertation hervorgegangen sind und bei denen ich Autor bin, entsprechen den URM und werden von mir verantwortet.

Die Bedeutung dieser eidesstattlichen Versicherung und die strafrechtlichen Folgen einer unwahren eidesstattlichen Versicherung (§156,161 des Strafgesetzbuches) sind mir bekannt und bewusst.

_____

Berlin, 27. April 2015   Elena Bros

ANTEILSERKLÄRUNG AN DEN ERFOLGTEN PUBLIKATIONEN

(statement of percent contribution)

Elena Bros hatte folgenden Anteil an den folgenden Publikationen:

Publikation 1: Bros H, Millward JM, Paul F, Niesner R, Infante-Duarte C, Oxidative damage to mitochondria at the nodes of Ranvier precedes axon degeneration in ex vivo transected axons, Experimental Neurology, 2014.

70 %; Beitrag im Einzelnen: Studiendesign und -planung, Etablierung des experimentellen ex vivo Modells, Durchführung der Studienmessungen, Datenauswertung und -interpretation, graphische Darstellung der Studienergebnisse, Erstellung und Revision des Manuskripts.

Publikation 2: Bros H, Hauser A, Paul F, Niesner R, Infante-Duarte C, Assessing mitochondrial movement within neurons: manual vs. automated tracking methods, Traffic, 2015.

80 %; Beitrag im Einzelnen: Studiendesign und -planung, Durchführung der Studienmessungen, Datenauswertung und -interpretation, graphische Darstellung der Studienergebnisse, Erstellung und Revision des Manuskripts, korrespondierende Autorin.

Publikation 3: Fiebiger SM, Bros H, Grobosch T, Janssen A, Chanvillard C, Paul F, Dorr J, Millward JM, Infante-Duarte C, The antioxidant idebenone fails to prevent or attenuate chronic experimental autoimmune encephalomyelitis in the mouse, Journal of Neuroimmunology, 2013.

20 %; Beitrag im Einzelnen: Mitarbeit am Versuchsdesign, Durchführung der LC-MS/MS Messungen, Auswertung, Interpretation und Darstellung der LC-MS/MS Ergebnisse, Unterstützung bei der Erstellung des Manuskripts und während des Begutachtungsprozesses.

Berlin, 27. April 2015

_____

PD Dr. Carmen Infante Duarte

_____

Elena Bros

DRUCKEXEMPLARE DER AUSGEWÄHLTEN PUBLIKATIONEN

(selected publications)

Fogende Originalartikel wurden aus Gründen des Copyright in der elektronischen Version meiner Arbeit nicht veröffentlicht:

Publication 1

Bros H, Millward JM, Paul F, Niesner R, Infante-Duarte C. **Oxidative damage to mitochondria at the nodes of Ranvier precedes axon degeneration in *ex vivo* transected axons**. Experimental Neurology, 2014. 261:127-35.

http://dx.doi.org/10.1016/j.expneurol.2014.06.018

Publication 2

Bros H, Hauser A, Paul F, Niesner R, Infante-Duarte C. **Assessing mitochondrial movement within neurons: manual vs. automated tracking methods**. Traffic, 2015. 16(8):906-17.

http://dx.doi.org/10.1111/tra.12291

Publication 3

Fiebiger SM, Bros H, Grobosch T, Janssen A, Chanvillard C, Paul F, Dorr J, Millward JM, Infante-Duarte C. **The antioxidant idebenone fails to prevent or attenuate chronic experimental autoimmune encephalomyelitis in the mouse.** Journal of Neuroimmunology, 2013. 15;262(1-2):66-71.

http://dx.doi.org/10.1016/j.jneuroim.2013.07.002

CURRICULUM VITAE

Mein Lebenslauf wird aus datenschutzrechtlichen Gründen in der elektronischen Version meiner Arbeit nicht veröffentlicht.

PUBLICATION LIST

Bros H, Hauser A, Paul F, Niesner R, Infante-Duarte C. Assessing mitochondrial movement within neurons: manual vs. automated tracking methods. Traffic. 2015 doi: 10.1111/tra.12291.

Janssen A, Fiebiger S, **Bros H**, Hertwig L, Romero-Suarez S, Hamann I, Chanvillard C, Bellmann-Strobl J, Paul F, Millward JM, Infante-Duarte C. Treatment of chronic experimental autoimmune encephalomyelitis with epigallocatechin-3-gallate and glatiramer acetate alters expression of heme-oxygenase-1. PLoS One. 2015. 26;10(6):e0130251. doi: 10.1371/journal.pone.0130251.

Bros H, Niesner R, Infante-Duarte C. An *ex vivo* model for studying mitochondrial trafficking in neurons. Methods Mol Biol. 2015;1264:465-72. doi: 10.1007/978-1-4939-2257-4_38.

Bros H, Millward JM, Paul F, Niesner R, Infante-Duarte C. Oxidative damage to mitochondria at the nodes of Ranvier precedes axon degeneration in *ex vivo* transected axons. Exp Neurol. 2014;261:127-35. doi: 10.1016/j.expneurol.2014.06.018.

Fiebiger SM, **Bros H**, Grobosch T, Janssen A, Chanvillard C, Paul F, Dörr J, Millward JM, Infante-Duarte C. The antioxidant idebenone fails to prevent or attenuate chronic experimental autoimmune encephalomyelitis in the mouse. J Neuroimmunol. 2013;262(1-2):66-71. doi: 10.1016/j.jneuroim.2013.07.002.

Galinovic I, Ostwaldt AC, Soemmer C, **Bros H**, Hotter B, Brunecker P, Fiebach JB. Automated vs manual delineations of regions of interest- a comparison in commercially available perfusion MRI software. BMC Med Imaging. 2012;12:16. doi: 10.1186/1471-2342-12-16.

Galinovic I, Ostwaldt AC, Soemmer C, **Bros H**, Hotter B, Brunecker P, Schmidt WU, Jungehülsing J, Fiebach JB. Search for a map and threshold in perfusion MRI to accurately predict tissue fate: a protocol for assessing lesion growth in patients with persistent vessel occlusion. Cerebrovasc Dis. 2011;32(2):186-93. doi: 10.1159/000328663.

ACKNOWLEDGMENTS